FERMILAB
NOV 11 1996
LIBRARY

Institut de Physique Nucléaire de Lyon

Université Claude Bernard

IN2P3 - CNRS

13

LYCEN 9628
Septembre 1996

LYCEN - 9628 -
Fermilab Library
0 1160 0045363 3

Mass distribution and multiple fragmentation events in high energy cluster-cluster collisions : evidence for a predicted phase transition

B. Farizon, M. Farizon, M.J. Gaillard, R. Genre, S. Louc, J. Martin

Institut de Physique Nucléaire de Lyon, IN2P3/CNRS, Université Claude Bernard,
F-69622 Villeurbanne Cedex, France

J.P. Buchet, M. Carré

Laboratoire de Spectrométrie Ionique et Moléculaire, Université Claude Bernard,
43 boulevard du 11 Novembre 1918, 69622 Villeurbanne Cedex, France

G. Senn, P. Scheir and T. D. Märk

Institut für Ionenphysik, Leopold Franzens Universität,
Technikerstr. 25, 6020 Innsbruck, Austria

Submitted to Phys. Rev. Lett.

43, Boulevard du 11 Novembre 1918 - 69622 VILLEURBANNE Cedex - France

MASS DISTRIBUTION AND MULTIPLE FRAGMENTATION EVENTS IN HIGH ENERGY CLUSTER-CLUSTER COLLISIONS: EVIDENCE FOR A PREDICTED PHASE TRANSITION

B. Farizon, M. Farizon, M.J. Gaillard, R. Genre, S. Louc, J. Martin
Institut de Physique Nucléaire de Lyon, IN2P3 - CNRS et Université Claude Bernard,
43, boulevard du 11 Novembre 1918, 69622 Villeurbanne Cedex, France

J.P. Buchet, M. Carré,
Laboratoire de Spectrométrie Ionique et Moléculaire, Université Claude Bernard,
43, boulevard du 11 Novembre 1918, 69622 Villeurbanne Cedex, France

G. Senn, P. Scheier and T.D. Märk
Institut für Ionenphysik, Leopold Franzens Universität,
Technikerstr.25, 6020 Innsbruck, Austria.

Abstract

Fragment size distributions including multiple fragmentation events have been measured for high energy H_{25}^{+} cluster ions (60 keV/amu) colliding with a neutral C_{60} target. In contrast to earlier collision experiments with a helium target the present studies do not show a U-shaped fragment mass distribution, but a single power-law falloff with increasing fragment mass. This behaviour is similar to what is known for the intermediate regime in nuclear collision physics and thus confirms a recently predicted scaling from nuclear to molecular collisions.

PACS numbers: 36.40.+d

Phys. Rev.Lett., submitted 30 July, shortened version 15th august 1996

Fragmentation of finite size systems such as nuclei, molecules and clusters has attracted much interest recently and one intriguing result of these studies is the recognition that the general features of this phenomenon are rather independent of the actual system studied [1]. Thus not surprisingly one important field in cluster science is the study of the fragmentation behaviour of excited cluster ions, X_n^{+*}, i.e.,

$$X_n^{z+*} \longrightarrow \Sigma X_p^{+} \qquad \text{(with } \Sigma\, p = n) \qquad (1)$$

produced by such diverse means as photon, electron, ion impact and surface collisions [2]. Whereas fragmentation induced by low energy deposition has been usually interpreted in the frame of the evaporative ensemble model [3-5,6], recently reported fragmentation patterns obtained in high energy collisions of hydrogen [7,8] and fullerene cluster [9, 10] ions showing bimodal (U-shaped) decay patterns (see Fig.1) have been interpreted by the occurrence of both evaporative cooling reactions and multifragmentation processes. Moreover, beam foil experiments with hydrogen cluster ions [11] have lead to a complete disintegration of the projectile yielding only atomic fragment ions X_1^+. All of these distribution patterns obtained in cluster ion fragmentation studies are similar to what has been also observed in nuclear fragmentation; see Fig.1 showing a schematic representation of the different decay patterns observed in nuclear reactions. The intermediate regime, however, which is characterized experimentally and theoretically in nuclear reactions by a fragment distribution (designated in nuclear physics as Intermediate Mass Fragments -IMF- and in Fig.1 as curve (3)) consisting solely by a decreasing function

$$Y_p \propto (p/n)^{-\tau} \qquad (2)$$

has so far not been observed in cluster experiments. As this intermediate regime is, however, of particular importance, because of the predicted presence of a critical behaviour in the case of nuclear fragmentation (i.e., liquid-gas phase transition in the fragmentation of hot reaction compounds [12-16]), the present study has been devoted to explore for the first time this fragmentation regime for the cluster case.

The present experiments were prompted by theoretical studies of Bonasera and coworkers predicting the scaling of this critical behaviour from nuclear to molecular collisions [16]. From these studies follows that in extending our previous work [7] involving the fragmentation of hydrogen cluster ions (with laboratory energies in the order of 60 keV/amu) via impact on a helium target to fragmentation studies with a C_{60} target, it should be possible -

due to the different energy deposition in the later case - to reach this intermediate regime. The present work not only gives the first experimental evidence for the existence of this intermediate regime in the case of cluster fragmentation (i.e., by not showing any increase in the fragmentation distribution at higher masses, see Fig.1), but also contains clear experimental proof for the multifragmentation character of the fragmentation mechanism characteristic for this regime. Detailed analysis of the decay patterns for both targets, helium and fullerene, shows (i) evidence for the general applicability of theoretical descriptions of fragmentation processes for finite systems as diverse as nuclei and clusters and (ii) by analogy to nuclear case [12-16] a first indication for a possible liquid-gas phase transition in the excited cluster ions during the decay reaction. Moreover, the present work also constitutes the first experiment involving reactive collisions between different mass selected clusters thus extending the previous cluster cluster collision (CCC) studies between fullerenes [17].

Mass-selected hydrogen cluster ions of 60 keV/amu are prepared in a high-energy cluster ion beam facility consisting of a cryogenic cluster jet expansion source combined with a high performance electron ionizer and a two-step ion accelerator (for details see [18-20]). After momentum analysis by a magnetic field, the mass selected and pulsed high energy projectile beam (pulse length of 100 ms; repetition frequency of 1 Hz) - consisting of H_{25}^+ in the present case - is collimated by two apertures ensuring an angular dispersion of about $\pm$ 0.8 mrad. This cluster ion projectile beam is crossed perpendiculary by a C_{60} effusive beam produced by evaporation of pure C_{60} powder in a single-chamber molybdenum oven (at about 675° C). The C_{60} beam constitutes for the fast cluster projectile ion beam a gas target of about 5×10^{12} C_{60} clusters per cm^2.

One meter behind the interaction region with the target the fast hydrogen collision products (neutrals and ions) are passing a magnetic sector field analyzer, the corresponding flight time being about 0.3 μs. Both, the undissociated H_{25}^+ cluster ions and the charged fragment ions H_p^+ are then detected with a multi-detector device consisting of several surface-barrier detectors located at different positions at the exit of the analyzer. This allows to record simultaneously and in coincidence neutral and various charged fragment products (for details see [20]). From the measured fraction of transmitted H_{25}^+ parent ions and the estimated C_{60} target thickness we obtain a total dissociation cross section of about 14×10^{-15} cm^2, a value which is as expected about an order of magnitude larger than the value of $(2.9 \pm 0.4) \times 10^{-15}$ cm^2 measured previously with a helium target at the same projectile velocity [6].

Fig.2 shows the normalized fragment ion yield Y_p (i.e., number of fragment ion H_p^+ divided by the total number of dissocated parent ions H_{25}^+) versus the normalized fragment size

p/25. Also shown for the same projectile and projectile velocity are our previous data [8] (including here also yields for the light fragment ions H_2^+ and H^+ not given in the Ref. [8]) obtained with a helium gas jet. Whereas fragmentation of H_{25}^+ with the helium target leads to a U-shaped fragment ion distribution, interaction with C_{60} exhibits a monotonously decreasing distribution typical for the IMF case known in nuclear physics, i.e., the increase at the higher p/n values due to reactions involving sequential evaporation of excited parent ions, present in the helium target case, is completely absent in collisions with C_{60}. In addition to this overall behaviour of the fragment distribution, size effects are clearly visible for the H_9^+ and H_{19}^+ fragment ions, the relative maxima in the $Y_{p=9 \text{ and } 19}$ yield being due to shell closure effects predicted in the structure of hydrogen cluster ions [21].

Most importantly, as can be seen in a log-log plot of these data in Fig.3 the overall Y_p distribution follows closely the power law given in equ.(2), yielding for the present case of a C_{60} target a τ of 2.56 when fitting the data for fragment sizes $23 \geq p \geq 3$. The yields for the two smallest fragment sizes H^+ and H_2^+ and the yield for H_{19}^+ have not been included in Fig.3 and this fitting procedure. Whereas in the case of H_{19}^+ due to a pronounced shell effect the measured yield is larger than that predicted from the power law, in the case of the two smallest fragments the data points are lying below the expected values. The latter can be explained by the fact that this power law applies to the total fragmentation yield irrespective of the charge of the fragments. As has been shown previously [19] about 70 % of the mass of the parent ion ends up in neutral fragments consisting mainly of H_2 and H.

As can be seen in Fig.3 our previous data obtained with a helium target also display a power law, but only in the lower mass portion of the distribution (i.e., from fragment size 3 to 11) with a τ of 2.63 [7]. Even more important, however, is that the present power law dependence is very similar to the IMF case in nuclear collisions where (i) the mass distribution follows equ.(2) with a τ value of equal to 2.6 for inclusive (impact parameter integrated) reactions [12] and where (ii) the fragmentation is associated with abundant multi-fragmentation events [22]. This latter rather characteristic feature of the nuclear fragmentation can be also observed in the present case (see Fig.4) thereby confirming (i) the similarity between these two different collision systems and (ii) thus the validity of the scaling law conjectured recently by Bonasera and Schulte [16].

Fig.4 gives the normalized fragment ion yield Y_p^m, for the smallest fragment ion H^+, where the multiplicity m is the number of fragments H_p^+ produced per collision. For comparison our previous results [23] concerning the helium target for the same projectile velocity are included in Fig.4. As can be seen from these data there appears a distinct difference for the two

targets. Both the multiplicity and the production probability are much larger for the C_{60} target, which is in line with the fact that in this case there is a larger energy deposition during the collision thereby leading to stronger multifragmentation in particular concerning proton production. It is interesting to note that in the earlier beam foil experiments with hydrogen cluster ions leading to a complete disintegration of the projectile ion a multiplicity for the proton production of up to 9 has been observed. Thus the data shown in Fig.4 clearly demonstrate the presence of multi-fragmentation events and their dependence on energy transfer, i.e., when increasing the energy deposition by going from the helium target to the C_{60} target. So, from a mass distribution (2) to (3) in Fig.1 both, the multiplicity and probability of proton production, increase strongly.

Both the change in the mass fragment distribution (and in particular the observation of a distribution following equ.(2) for the C_{60} target) and the increase in multiple fragment ion production can be discussed in light of recent studies by Bonasera and coworkers [14,16,24]. These authors have argued that one prerequisite for the occurrence of a critical behaviour of a finite classical system such as a liquid-gas phase transition during the fragmentation of hot nuclear matter (accompanied by the formation of many fragments in the final stage of the reaction) is the observation of a power law in the fragment mass distribution according to equ.(2). Such a power law with a τ of 2.23 is expected for condensation near the critical temperature indicating thus a liquid-gas phase transition as described by the droplet model of Fisher [25]. As a matter of fact as they increase the temperature in their finite classical systems [14] in order to reach this critical behaviour regime they observe with increasing temperature a similar transition in the fragment mass distributions as when going in the present case from the helium to the fullerene target. Based on this and on a recent theoretical study of these authors about the possibility of scaling of this critical behaviour from nuclear collisions to molecular collisions [16] we can conclude that we have demonstrated in the present study experimentally the occurrence of at least one rather characteristic fingerprint of this behaviour in the case of cluster cluster collisions.

In concluding, the present results show (i) convincing evidence for the general applicability of the same theoretical description and possible interpretation of fragmentation for such diverse systems as nuclei and clusters and by this (ii) a first indication for the possible presence of a phase transition and concomitant instabilities (as shown to be present in nuclear reactions with similar fragmentation features) in the excited cluster ions during the decay reaction.

Acknowledgements.

Work partially supported by the Österreichische Fonds zur Förderung der Wissenschaftlichen Forschung, Wien, Austria. The Laboratoire de Spectrométrie Ionique et Moléculaire is an Unité Mixte de Recherche de l'Université Lyon I et du CNRS (UMR 5579). The Institut de Physique Nucléaire de Lyon is an Unité Mixte de Recherche de l'Université Lyon I et du CNRS (UMR 5822)

REFERENCES

[1] D. Beysens, X.Campi and E. Pfefferkorn (Eds.), Fragmentation Phenomena, Les Houches Series, World Scientific, Singapure, 1995

[2] International cluster workshop, Col de Porte, 6-9 Febr. 1996

[3] C.E. Klots, J. Phys. Chem., 92 (1988) 5864

[4] T.D. Märk, in Linking the Gaseaous and Condensed Phases of Matter, L.G. Christophorou, E. Illenberger, W.F. Schmidt, EDS, Plenum, NewYork, 1994

[5] R. Wörgötter, B. Dünser, P. Scheier, T.D. Märk, M. Foltin, C.E. Klots,J. Laskin, C. Lifshitz, J. Chem. Phys. 104 (1996) 1225

[6] A. Van Lumig and J. Reuss, Int. J. Mass Spectrom. Ion Phys., 27 (1978) 197

[7] B. Farizon, M. Farizon, M.J. Gaillard, E. Gerlic et S. Ouaskit, Nucl. Instr. Meth. B88 (1994) 86

[8] S. Ouaskit, B. Farizon, M. Farizon, M.J. Gaillard, A. Chevarier, N. Chevarier, E. Gerlic and M. Stern, Int. J. Mass Spectrom. Ion Proc.,139 (1994) 141

[9] T. LeBrun, H.G. Berry, S. Cheng, R.W. Dunford, H. Esbensen, D.S. Gemmell, E.P. Kanter, W. Bauer, Phys. Rev. Lett. 72, 3965 (1994).

[10] R. Ehlich, M. Westerburg, and E.E.B. Campbell, J. Chem. Phys. 104, (1996) 1900

[11] B. Mazuy, A. Belkacem, M. Chevallier, M.J. Gaillard, J.C. Poizat, J. Remillieux, Nucl. Instrum. Meth., B28 (1987) 497

[12] X. Campi, Proceedings of the 107th Course of the Int. School of Physics "Enrico Fermi" on the Chemical Physics of Atomic and Molecular Clusters (Varenna 1988); Nucl. Phys. A545 (1992) 161

[13] D.H.E. Gross, A.R. De Angelis, H.R. Jaqaman, Pan Jicai, and R. Heck, Phys. Rev. Lett. 68 (1992) 146

[14] V. Latora, M. Belkacem and A. Bonasera, Phys. Rev. Lett. 73 (1994) 1765

[15] D.H.E. Gross, P.A. Hervieux, Z. Phys. D 35 (1995) 27

[16] A. Bonasera and J. Schulte,
Report n° MSUCL-966 (1996)

[17] E.E.B. Campbell, V. Schyja, R. Ehlich and I.V. Hertel,
Phys. Rev. Lett. 70 (1993) 263

[18] M.J. Gaillard, A. Schempp, H.O. Moser, H. Deitinghoff, R. Genre, G. Hadinger, A. Kipper, J. Madlung, J. Martin, Proceedings of ISSPIC 6, Chicago (1992), Z. Phys. D 26 (1993) S347

[19] B. Farizon, M. Farizon, M.J. Gaillard, E. Gerlic and S. Ouaskit, Int. J. Mass Spectrom. Ion Proc.144 (1995) 79

[20] B. Farizon, M. Farizon, M.J. Gaillard, E. Gerlic, R. Genre, S. Louc, N.V.de Castro Faria and G.Jalbert,
Chem. Phys. Lett. 252 (1996) 147

[21] M. Farizon, H. Chermette, and B. Farizon Mazuy,
J. Chem. Phys. 96 (1992) 1325

[22] A. Hirsch et al.,
Phys. Rev. C29 (1984) 508

[23] B. Farizon, M. Farizon, M.J. Gaillard, E. Gerlic et S. Ouaskit,
Z. Phys. D 33 (1995) 53

[24] M. Belkacem, V. Latora and A. Bonasera, Critical evolution of a finite system,
preprint LNS

[25] M.E. Fisher,
Rep. Prog. Phys. 30 (1967) 615

FIGURE HEADINGS

Fig.1 Schematic representation of normalized fragmentation yield versus normalized fragment size p/n. (1) Low energy collisions between H_{25}^+ cluster ions and atoms after Reuss and coworkers [6]; (2) High energy collisions between cluster ions and He atoms after [7-9]; (3) High energy collisions between cluster ions and C_{60} ; and (4) High energy beam foil collision experiment with cluster ions after [11].

Fig.2 Measured normalized fragment ion yield Y_p versus normalized fragment size p/25 for H_{25}^+ projectile ions interacting at 1.5 MeV collision energy with a helium or C_{60} target, respectively.

Fig.3 Log-log plot of normalized fragment ion distributions for H_{25}^+ projectile ions interacting at 1.5 MeV collision energy with helium or C_{60} target, respectively demonstrating the power law behaviour of the data selected (see text).

Fig.4 Normalized H^+ fragment ion yield versus multiplicity of fragment ion production for H_{25}^+ projectile ions for a helium or C_{60} target.

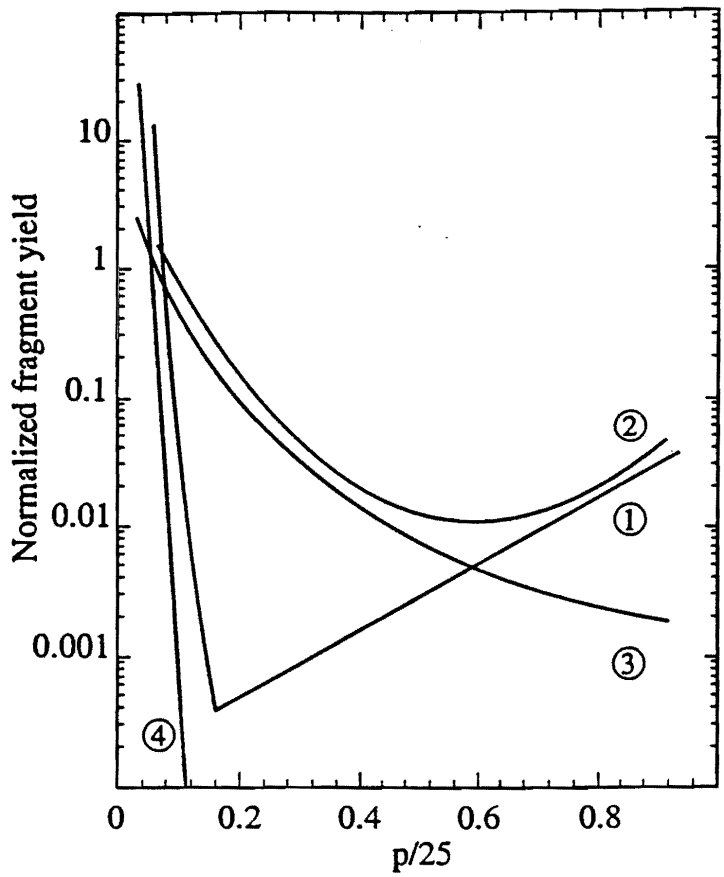
Normalized fragment yield
10
1
0.1
0.01
0.001
0
0.2
0.4
0.6
0.8
p/25
②
①
③
④

Figure 1

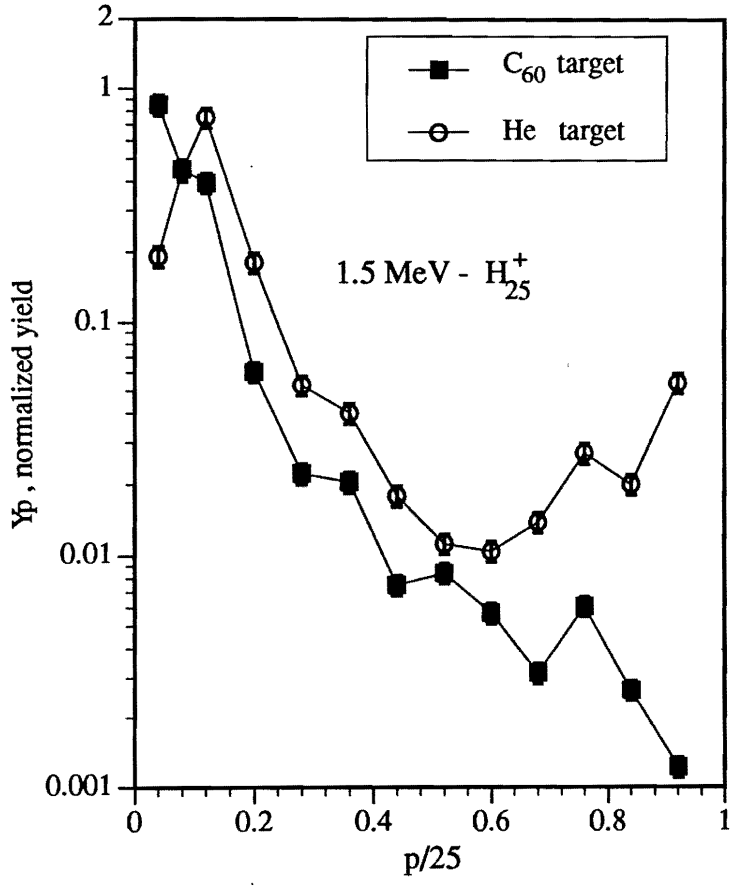
2
1
0.1
0.01
0.001
0
0.2
0.4
0.6
0.8
1
p/25
Yp , normalized yield
C60 target
He target
1.5 MeV - H+25

Figure 2

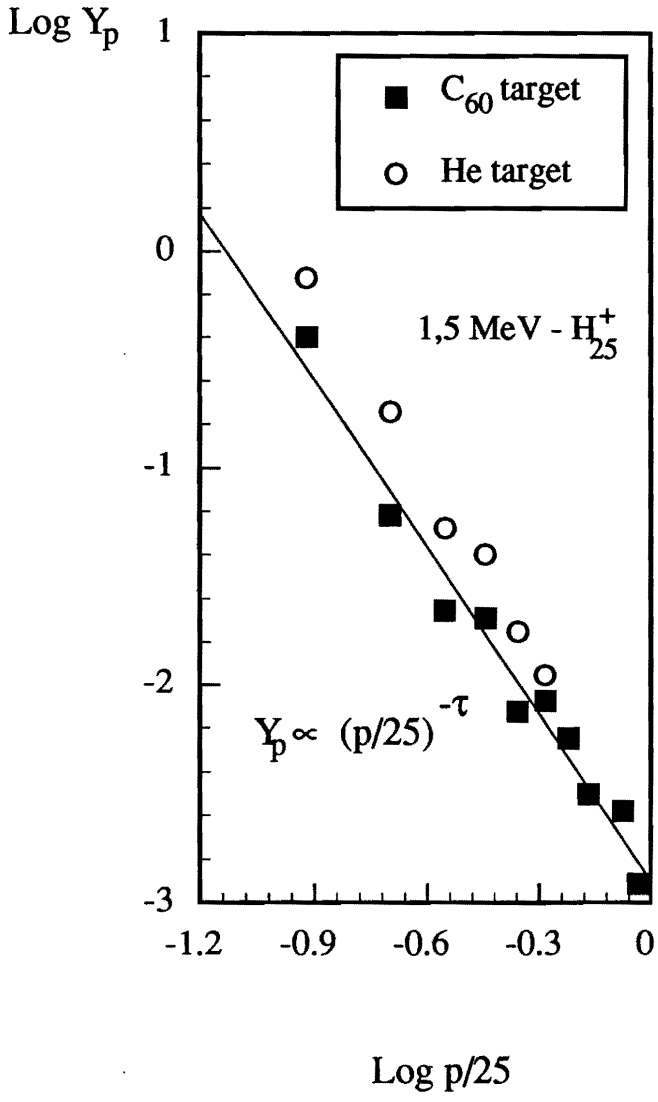
Log Y_p
1
0
-1
-2
-3
-1.2
-0.9
-0.6
-0.3
0
C_{60} target
He target
1,5 MeV - H^+_{25}
$Y_p \propto (p/25)^{-\tau}$
Log p/25

Figure 3

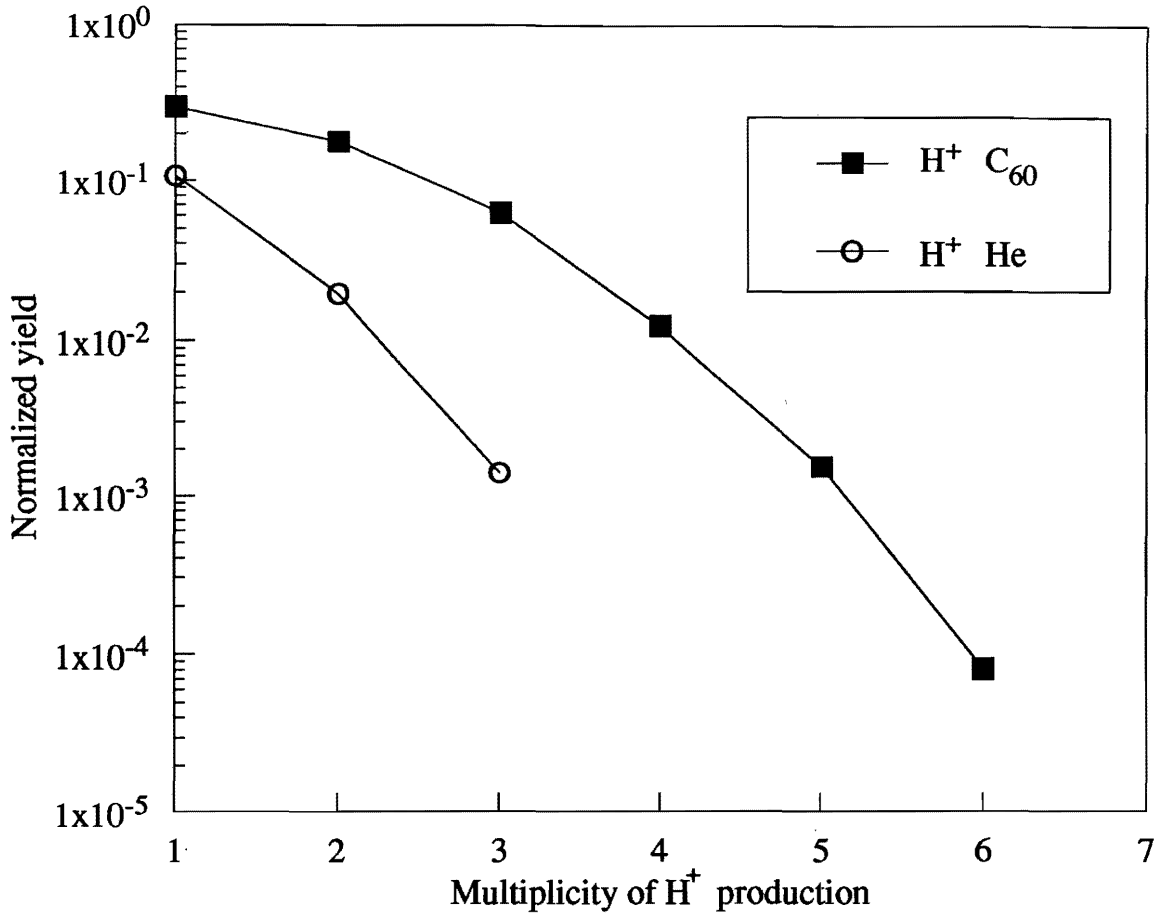
1x10^0
1x10^-1
1x10^-2
1x10^-3
1x10^-4
1x10^-5
Normalized yield
1
2
3
4
5
6
7
Multiplicity of H+ production
H+ C60
H+ He

Figure 4